

Published in final edited form as:

Clin Cancer Res. 2015 May 15; 21(10): 2297–2304. doi:10.1158/1078-0432.CCR-14-3258.

The c-Met tyrosine kinase inhibitor JNJ-38877605 causes renal toxicity through species specific insoluble metabolite formation

Martijn P. Lolkema^{#1,3}, Hilde H. Bohets^{#2}, Hendrik-Tobias Arkenau¹, Ann Lampo², Erio Barale², Maja J.A. de Jonge³, Leni van Doorn³, Peter Hellemans², Johann S. de Bono¹, and Ferry A.L.M. Eskens³

¹Phase I Unit, Royal Marsden NHS Foundation Trust, Surrey & London, United Kingdom

²Janssen Research and Development, Beerse, Belgium ³Dept. of medical Oncology, Erasmus MC Cancer Institute Rotterdam, The Netherlands

These authors contributed equally to this work.

Summary

Purpose—The receptor tyrosine kinase c-Met plays an important role in tumorigenesis and is a novel target for anti-cancer treatment. This phase I, first-in-human trial, explored safety, pharmacokinetics, pharmacodynamics and initial antitumor activity of JNJ-38877605, a potent and selective c-Met inhibitor.

Experimental design—We performed a phase I dose escalation study according to the standard 3+3 design.

Results—Even at sub-therapeutic doses, mild though recurrent renal toxicity was observed in virtually all patients. Renal toxicity had not been observed in preclinical studies in rats and dogs. Additional preclinical studies pointed towards the rabbit as a suitable toxicology model, as the formation of the M10 metabolite of JNJ-38877605 specifically occurred in rabbits and humans. Additional toxicology studies in rabbits clearly demonstrated that JNJ-38877605 induced species specific renal toxicity. Histopathological evaluation in rabbits revealed renal crystal formation with degenerative and inflammatory changes. Identification of the components of these renal crystals revealed M1/3 and M5/6 metabolites. Accordingly, it was found that humans and rabbits showed significantly increased systemic exposure to these metabolites relative to other species. These main culprit insoluble metabolites were generated by aldehyde oxidase activity. Alternative dosing schedules of JNJ-38877605 and concomitant probenecid administration in rabbits failed to prevent renal toxicity at dose levels that could be pharmacologically active.

Correspondence to: Martijn P. Lolkema, MD, PhD, m.lokema@erasmusmc.nl, PO Box 5201, 3008AE Rotterdam, The Netherlands, Tel: +31107041906, Fax: +31107041003.

Study is listed on www.clinicaltrials.gov website: identifier: NCT00651365

Conflict of Interest:

Hilde H. Bohets PhD, Ann Lampo DVM, Erio Barale DVM and Peter Hellemans MD are employees of Janssen Research and Development, Belgium and Hilde H. Bohets PhD, Ann Lampo DVM, and Peter Hellemans MD hold stocks in Johnson & Johnson. Janssen Research and Development is a member of the Janssen Pharmaceutical Companies.

Conclusion—Combined clinical and correlative preclinical studies suggest that renal toxicity of JNJ-38877605 is caused by the formation of species specific insoluble metabolites. These observations preclude further clinical development of JNJ-38877605.

Keywords

c-Met; receptor tyrosine kinase inhibitor; phase I study; nephrotoxicity; aldehyde oxidase; metabolism; crystal metabolites

Introduction

Tumor cell migration, invasiveness and metastasis formation are important therapeutic targets in oncology drug development. The hepatocyte growth factor (HGF), also known as scatter factor, and its receptor c-Met, play an important role in physiological processes such as embryological development, wound healing, tissue regeneration, angiogenesis, cell growth, local invasion and morphogenetic differentiation (1). In physiological and pathophysiological situations HGF is primarily produced by fibroblast like cells, whereas c-Met is expressed by epithelial cells. Aberrant expression of c-Met is involved in tumor progression (2, 3). Activating c-Met mutations have been identified in hereditary and sporadic papillary kidney cancer and gastric carcinomas, suggesting a potential causal role for c-Met activation in tumorigenesis (4, 5). Moreover c-Met amplification is a well-known event in non-small cell lung cancer especially important in resistance to EGFR inhibition (6). In a small subset of glioblastoma multiforme patients activating c-Met mutations have been reported and activation of the HGF-c-Met axis seems to play a role in resistance to therapy (7). Therefore, inhibiting the activity of c-Met is a relevant objective in anti-cancer drug development.

JNJ-38877605 is an orally available, nanomolar active (IC_{50} 4.7 nM for c-Met Kinase *in vitro*) and highly selective c-Met ATP competitive kinase inhibitor (8). JNJ-38877605 inhibits c-Met kinase with >833 fold selectivity relative to the next most potently inhibited kinase (Fms) of 246 kinases tested. JNJ-38877605 binds to the ATP binding site of c-Met kinase with a high affinity that leads to a slow reversibility of binding. JNJ-38877605 has shown a favorable safety profile in rat and dog studies and demonstrated anti-tumor activity in xenograft models of prostate, non-small cell lung and gastric cancer as well as in glioblastoma models.

This phase I, open-label, dose-escalation study explored safety, tolerability and pharmacokinetics of orally administered JNJ-38877605.

Methods

Patients and eligibility criteria

This was a non-randomized, open-label, phase 1, dose-escalation study conducted at two participating institutions. The study was conducted in accordance with the International Conference on Harmonization Good Clinical Practice, in accordance with the ethical principles of the current Declaration of Helsinki and was approved by both institutional Ethics committees. All patients provided written informed consent before any study-related

procedures were performed. All patients fulfilled the eligibility criteria (Supplemental methods). The population was a standard first-in-human oncology phase I study population (Supplemental table 1).

Treatment Administration

Screening was performed according to protocol (Supplemental methods). The study was designed to determine the Maximum Tolerated Dose (MTD) for orally administered JNJ38877605. The compound was manufactured according to GMP standards and supplied by Janssen Research and Development.

Selection of the Safe Starting Dose for the Clinical Study

The starting dose of 60 mg once daily (OD) for continuous daily administration was calculated based upon current recommendations for first-in-human Oncology studies in accordance with the recent EMEA (European Medicines Evaluation Agency) guideline on strategies to identify and mitigate risks for first-in-human clinical trials with investigational medicinal products (details: Supplemental methods).

Toxicity Assessments

Toxicities were graded according to the Common Terminology Criteria for Adverse Events (CTCAE) version 3.0 and safety assessments were performed according to protocol (Supplementary methods). Dose Limiting Toxicity (DLT) was defined using standard criteria (Supplemental methods)

Determination of Maximal Tolerated Dose (MTD)

If 0 out of 3 patients experienced DLT during the first 21 day treatment cycle, dose escalation could be pursued according to protocol. If 1 out of 3 patients experienced DLT during the first treatment cycle, up to 3 additional patients were to be treated at that dose level. The MTD was defined as the highest dose level at which fewer than 2 out of 6 patients experienced DLT.

Pharmacokinetics (PK)

Blood samples were taken at pre-specified times (see Supplemental methods) and analyzed quantitatively for JNJ-38877605 and the N-desmethyl metabolite, M2. For both compounds, C_{max}, time to C_{max} (t_{max}), elimination half life time (t_{1/2}), area under the plasma concentration curve (AUC) and terminal elimination rate were calculated.

Toxicology studies in the model organisms

Toxicology studies were performed according to ICH Topic S9. Nonclinical Evaluation for Anticancer Pharmaceuticals, EMEA/CHMP/ICH/646107/2008, and ICH guideline M3(R2) on non-clinical safety studies for the conduct of human clinical trials and marketing authorization for pharmaceuticals. Initially male and female rats and dogs were chosen as toxicology species. The choice of the toxicology species is based on a comparison of the metabolism pattern in hepatocytes of preclinical species and man. Human metabolites should be covered in the toxicology species in order to assess compound and metabolite

related toxicity during the 1-month GLP toxicology study. Based on metabolite patterns in hepatocytes all human metabolites were present in rat and dog with the exception of an *N*-glucuronide, which is considered to be non-toxic. Therefore, rat and dog were identified as suitable species to test toxicity.

Following the observation of renal toxicity in the clinical study we chose rabbits because of the presence of the glucuronide of the desmethylmetabolite (M10) in rabbit and man, only. A 1-month non-GLP toxicology study of JNJ-38877605 was performed in the male rabbit and histopathological evaluation of the kidney was performed as well as all other standard tissue testing and sampling. In order to find possibilities to circumvent renal toxicity, various intermittent dosing schedules were explored (see table 1 for the dosing regimen and total weekly dose).

Metabolite identification

Metabolites were determined from in vitro systems (hepatocytes and liver subcellular fractions), and in vivo samples (plasma, urine and kidney samples). Metabolite identification was performed by LC-MS, quantitative data are only available for those metabolites with a reference standard or metabolites with a ³H label. Solubility measurements were performed for some of the metabolites.

Isoenzymes involved in the formation of the metabolites

Isoenzyme identification was performed with liver subcellular fractions. Isoenzymes involved in the metabolism of JNJ-38877605 were determined based on structural characteristics and after incubation with specific inhibitors of cytochrome P-450 and aldehyde oxidase (9).

Histopathological evaluation

Rabbit kidneys were fixed by formalin immersion, then processed routinely: trimming, embedding, sectioning at 3-5 µm, staining with hematoxylin and eosin (HE) and examined under bright field. Additional frozen sections of kidney were prepared and counterstained with either methylene blue or Von Kossa (to detect mineralization). They were examined under bright field and polarization microscopy.

Identification of the crystal structures in the kidneys

Kidney crystals detected under polarization microscopy were observed and analyzed in situ using Raman microscopy. Thereafter, they were harvested and analyzed with LC-MS.

Prevention of renal toxicity

A mechanistic study was performed to investigate the potential protective effect of probenecid on renal toxicity. Probenecid is known as a competitive inhibitor of organic acid transport in the kidney and other organs (10). After exposure to JNJ-38877605 in combination with probenecid, determination of pharmacokinetics (plasma, kidney, urine) of JNJ-38877605, renal parameters (blood urea nitrogen and creatinine) and kidney histopathology were performed in male rabbits.

Results

Toxicity in the phase I, first in human study of JNJ-38877605

A total of 5 subjects were enrolled in the first cohort of 60 mg OD. All subjects experienced a rapid, though asymptomatic Grade 1 serum creatinine (SCr) increase; in 4 patients this occurred as early as 2-3 days after the start of treatment, whereas 1 patient completed 4 weeks of treatment prior to SCr increase. In all cases treatment was interrupted. In 1 patient a re-challenge with JNJ-38877605 at the same dose was pursued after a 3-day interruption of therapy and subsequent normalization of SCr; this patient again experienced a grade 1 SCr increase after which treatment was permanently discontinued. All subjects recovered from their SCr increase after permanent treatment discontinuation. Cystatin C and blood urea nitrogen showed a comparable pattern to SCr, whereas calculated creatinine clearance decreased accordingly in 4 patients (Figure 1A/B).

To explore potential safe dose levels, an amendment was pursued allowing for dose levels of 10-40 mg OD to be explored. While 10 and 20 mg OD appeared to be safe with no indication of renal toxicity, at 40 mg OD again a rapid though asymptomatic grade 1 SCr increase was observed in 2/3 patients. It was then decided to discontinue further enrolment. During this part of the study glomerular filtration rate determination by Cr51 measurement was pursued in 1 patient in the 40mg cohort showing a >50% decrease (98 ml/min/1.73m² pre-treatment to 45 ml/min/1.73m² on cycle 1 day 21).

Pharmacokinetic analysis of JNJ38877605 in humans

JNJ38877605 was rapidly absorbed and showed a C_{max} at 1.5-4hr after ingestion (Figure 1C). A short plasma half-life and virtually no accumulation after 21 days was found. Comparison of plasma concentrations and AUC values over the different dosing cohorts showed dose proportionality (Supplemental table 2). At 60 mg OD, plasma concentrations and AUC did not reach levels that in preclinical models resulted in antitumor activity.

Inter-species difference in metabolism of JNJ-38877605

Based on a previous inter-species comparison of its metabolism, it was hypothesized that the renal toxicity of JNJ-38877605 that already occurred at sub-therapeutic doses, could possibly be explained by species specific metabolism. After incubation of JNJ-38877605 with liver fractions and identification of the metabolites with LC/MS-MS, several metabolites were observed. The major metabolic pathways in humans were demethylation, leading to M2, that was further metabolized to M5/M6 by hydroxylation of the quinoline moiety and to M10 by glucuronidation. JNJ-38877605 was also hydroxylated at the quinoline moiety to M1/M3. (Figure 2, Supplemental table 3). A comparative metabolism study in hepatocytes of rat, dog, rabbit and man showed a species-dependent formation of M10 (major in man and rabbit) and M11 (minor) (Supplemental figure 1). We therefore hypothesized that M10 could play a role in the observed clinical renal toxicity and subsequently selected rabbit as a toxicity model.

Renal effects after JNJ-38877605 administration during 1 month in rabbits

After total weekly intake of 200, 300 and 350 mg/kg/week for 1 month, creatinine clearance and several other chemistry parameters started changing. At necropsy (Table 1), rabbit kidneys showed increased weights (groups 3-6) and appeared pale (groups 4-6). Histopathological evaluation showed an extensive and prominent degeneration with inflammation, congestion, fibrosis, regeneration, and granular and acicular clefts sometimes surrounded by giant cells (Table 1; Figure 3B-D). In frozen sections examined under polarization microscopy, these clefts proved to be bi-refracting crystalline granules and spicules (Figure 3E/F). Some of the observed changes, in particular the kidney weight changes and the crystal accumulation, were still present after a 1-month recovery period (Supplemental table 4), with a moderate increase in urea nitrogen and a slight increase in creatinine.

As renal crystal formation was probably related to the formation of insoluble metabolites of JNJ-38877605 in the urine, we explored the potential protective effect of co-administration of probenecid. As probenecid is a competitive inhibitor of organic acid transport in the kidney and other organs, we hypothesized that it could block the renal transport of JNJ-38877605 and its metabolites. In a 7-day rabbit study, probenecid co-administration, however, resulted in more severe clinical observations compared to dosing with JNJ-38877605 alone and in similar histopathological changes (Supplemental table 5). In addition, exposure to JNJ-38877605 decreased after probenecid co-administration (data not shown).

Identification of the JNJ-38877605 derived metabolites in the renal crystals

We next harvested crystals from open slides without coverslips and analyzed those with LC-mass spectrometry; two chemical structures were proposed based on LC-MS results. Additional comparison of the LC-mass UV data with TOX LC-mass UV data and UV reference spectra allowed for the conclusion that both proposed structures contain a 2-hydroxyquinoline chromophore, with proposed structure 1 relating to JNJ-38877605 metabolites M5, M6 and proposed structure 2 relating to metabolites M1, M3. Additional experiments showed that the M5 metabolite displayed poor solubility at with a maximum concentration of 2-3 µg/ml solute over a range of pH.

We next performed mass balance studies in rats, dogs and rabbits showing that the excretion of JNJ-38877605 and its metabolites occurs partly through the kidney and rabbits and humans pre-dominantly excrete M3 and M5 in the urine. In rabbit urinary excretion was more important compared to rat and dog (data not shown). Plasma profiling showed a much lower abundance of M3 and M5 in rat and dog compared to rabbit and human (Table 2). These data suggested that plasma levels of M3 and M5 and their renal excretion play a critical role in the explanation of the renal findings.

Identification of the isoenzymes involved

Identification of the isoenzymes involved in the metabolism of JNJ38877605 is based on studies with specific inhibitors in liver microsomes and supernatant fractions. M3 is the most important metabolite formed after incubation of JNJ-38877605 with human liver

supernatant and is almost undetectable in human liver microsomes (Table 3a). This suggests that M3 is primarily formed by cytosolic enzymes. This is further corroborated by the fact that quercetin completely inhibited the formation of M3 in 12000×g fractions (Table 3b). Quercetin is a potent inhibitor of molybdenum hydroxylases like xanthine oxidase and aldehyde oxidase. Aldehyde oxidase is known to oxidize quinoline moieties, therefore most probably aldehyde oxidase and not xanthine oxidase is involved in the metabolism of JNJ-38877605. In addition, 1-aminobenzotriazole, a general cytochrome P-450 inhibitor, barely inhibits the M3 formation which is in line with the assumptions above (Table 3b). Cytochrome P-450 3A4 is clearly involved in the formation of the other metabolites. M5, the equivalent of M3 but originated from the demethylated JNJ-38877605 (M2) was not formed in microsomes or 12000×g. Based on the structural similarity with M3, it is assumed that it is also formed by aldehyde oxidase.

Discussion

In this first-in-human phase I study with the c-Met tyrosine kinase inhibitor JNJ-38877605 renal toxicity, hampering continuation of treatment, was observed after a short timeframe and at virtually all, even sub-therapeutic dose levels. Based upon the at that time available results from preclinical studies performed in mice, rats and dogs, this renal toxicity had not been foreseen. Extensive additional pre-clinical research therefore was initiated. Based on the subsequent analysis of metabolism data, the rabbit was subsequently identified as a relevant toxicity model. In this model we were able to recognize aldehyde oxidase-dependent and species-specific formation of insoluble metabolites that induced renal toxicity through precipitation of insoluble crystals in the renal tubules.

In the clinical study, although strongly and repeatedly considered, it was decided not to perform renal biopsies in any of the patients, and therefore the presence of such crystals in any of our patients could not be confirmed. This decision was based upon the clinical and ethical consideration that patients in this study had only asymptomatic Grade 1 serum creatinine (SCr) increases.

Unfortunately, we were not able to come up with a viable strategy to circumvent renal toxicity in the subsequently performed rabbit studies, and therefore it was decided that further clinical development of JNJ-38877605 had to be stopped.

With regard to the observed clinical toxicity of JNJ-38877605, it is intriguing that seemingly comparable observations were made in a phase I study with SGX523, another ATP competitive small molecule c-Met inhibitor (11). At doses exceeding 80 mg renal toxicity consisting of early rises in BUN and creatinine and obstructive nephropathy were observed. SGX523 equally showed a clean toxicity profile in rat and dog. SGX523 induced renal toxicity was considered probably related to the formation of two insoluble metabolites which were not formed in rat and dog. Subsequent studies performed in monkeys revealed the formation of crystals within renal tubules. The major urine metabolites in monkey were 2-quinolinone-SGX523 and the desmethyl metabolite of 2-quinolinone-SGX523. Both metabolites were also important in plasma. Metabolites were formed by aldehyde oxidase.

2-quinolinone-SGX523 was formed to a much lesser extent in rat and was absent in dog S-9 incubations (12).

The nephrotoxic metabolites could be detected in all hepatocytes cultures thus confounding the early signs of potential species specific generation. One hypothesis would be that they are formed by enzyme activity in the kidney. This hypothesis is corroborated by the lack of efficacy of probenecid. It is reported that the proximal, distal and collecting ducts of the kidney express aldehyde oxidase (13). Species specific aldehyde oxidase activity may contribute to the observed differences: in humans its activity is relatively high compared to rats and dogs (14). More conventional renal protective strategies such as hyper-hydration and furosemide co-administration were considered less suitable as we aimed for chronic administration of JNJ-38877605. In addition, above a certain level insoluble metabolites of JNJ-38877605 precipitate in the kidney and cannot be washed out.

Oxidation at the quinoline moiety can be mediated by aldehyde oxidase, as suggested by experiments with liver subcellular fractions. M3 is the most important metabolite formed after incubation of JNJ-38877605 with human liver subcellular fractions but almost undetectable in human liver microsomes, suggesting that M3 is primarily formed by cytosolic enzymes such as aldehyde oxidase. An inhibition experiment with quercetin (9, 15) in liver subcellular fractions further supported the involvement of aldehyde oxidase in the formation of M3.

Our observations strongly suggest that the observed renal toxicity of JNJ-38877605 is due to species specific metabolism and is not on target c-Met inhibitory effect. Several selective c-Met inhibitors have been tested in patients. Examples of well-tolerated small molecule c-Met inhibitors are INC280, volitinib (unpublished data) and foretinib (16). In addition, inhibiting HGF mediated signaling through the monoclonal antibodies rilotumumab and onartuzumab does not result in renal toxicity (17, 18). Thus, c-Met inhibition by itself is unlikely to induce on-target renal toxicity. SGX523, a structurally related small molecule c-Met inhibitor did induce a comparable spectrum of renal toxicity, which also prompted investigators to interrupt further clinical development (11, 12). These data underpin our observation that quinoline-containing chemical structures can be metabolized in a species-specific manner to form nephrotoxic poorly soluble metabolites explaining the observed renal toxicity of SGX523 and JNJ-38877605.

Revealing rabbit as an appropriate model system allowed us to explore potential strategies to circumvent the renal toxicity. Unfortunately, neither alternative scheduling of JNJ-38877605 nor probenecid co-administration proved to be a successful strategy in preventing renal toxicity. A potential strategy we have not explored is inhibiting aldehyde oxidase itself. A list of 239 drugs inhibiting aldehyde oxidase has been reported (19). Raloxifene is one of these inhibitors of aldehyde oxidase (IC_{50} value of 0.0029 μ M), and therefore, combining JNJ-38877605 with raloxifene could have been considered another preventive strategy to try to circumvent renal toxicity caused by JNJ-38877605.

In conclusion, JNJ-38877605 is an orally available, nanomolar active (IC_{50} 4.7 nM for c-Met Kinase in vitro) and highly selective c-Met ATP competitive kinase inhibitor whose

clinical activity was hampered by unexpected renal toxicity. Combined clinical and correlative preclinical studies suggest that this renal toxicity is caused by the formation of species specific insoluble metabolites that specifically occurs in rabbits and humans. These observations preclude further clinical development of JNJ-38877605.

Supplementary Material

Refer to Web version on PubMed Central for supplementary material.

Acknowledgements

The authors wish to thank all the patients, nurses, and site staff who participated in the study. Finally, the authors want to thank the compound development leader Peter Palmer, all collaborators of the preclinical toxicology, PDMS and pharmacokinetics departments for their dedication to the project, more specifically Tom Peeters, Petra Vinken Sofie Starckx, Dirk Cleeren, John Vandenberghe, Loes Versmissen, Kristel Buyens Hilde De Man, Katerijne Anciaux, Ellen Scheers, Carine Borgmans, Jan Snoeys Sandy Thijssen, Ludy van Beijsterveldt and Brendan Rooney.

Financial support:

We acknowledge support from Cancer Research UK for the ICR/RM cancer Centre; ECMC Centre support; and support to the Royal Marsden for the Biomedical Research Centre from the Department of Health in the UK. M.P. Lolkema has received a Dutch Cancer Foundation Fellowship grant (UU2008-4380) to support this work.

References

- Gentile A, Trusolino L, Comoglio PM. The Met tyrosine kinase receptor in development and cancer. *Cancer Metastasis Rev.* 2008; 27:85–94. [PubMed: 18175071]
- Kankuri E, Cholujoja D, Comajova M, Vaheri A, Bizik J. Induction of hepatocyte growth factor/scatter factor by fibroblast clustering directly promotes tumor cell invasiveness. *Cancer Res.* 2005; 65:9914–22. [PubMed: 16267016]
- Thiery JP. Epithelial-mesenchymal transitions in tumour progression. *Nat Rev Cancer.* 2002; 2:442–54. [PubMed: 12189386]
- Jeffers M, Schmidt L, Nakaigawa N, Webb CP, Weirich G, Kishida T, et al. Activating mutations for the met tyrosine kinase receptor in human cancer. *Proc Natl Acad Sci U S A.* 1997; 94:11445–50. [PubMed: 9326629]
- Lee JH, Han SU, Cho H, Jennings B, Gerrard B, Dean M, et al. A novel germ line juxtamembrane Met mutation in human gastric cancer. *Oncogene.* 2000; 19:4947–53. [PubMed: 11042681]
- Engelman JA, Zejnullahu K, Mitsudomi T, Song Y, Hyland C, Park JO, et al. MET amplification leads to gefitinib resistance in lung cancer by activating ERBB3 signaling. *Science.* 2007; 316:1039–43. [PubMed: 17463250]
- Boccaccio C, Comoglio PM. The MET oncogene in glioblastoma stem cells: implications as a diagnostic marker and a therapeutic target. *Cancer Res.* 2013; 73:3193–9. [PubMed: 23695554]
- Benvenuti S, Lazzari L, Arnesano A, Li Chiavi G, Gentile A, Comoglio PM. Ron kinase transphosphorylation sustains MET oncogene addiction. *Cancer Res.* 2011; 71:1945–55. [PubMed: 21212418]
- Kitamura S, Sugihara K, Ohta S. Drug-metabolizing ability of molybdenum hydroxylases. *Drug Metab Pharmacokinet.* 2006; 21:83–98. [PubMed: 16702728]
- Cunningham RF, Israili ZH, Dayton PG. Clinical pharmacokinetics of probenecid. *Clin Pharmacokinet.* 1981; 6:135–51. [PubMed: 7011657]
- Infante JR, Rugg T, Gordon M, Rooney I, Rosen L, Zeh K, et al. Unexpected renal toxicity associated with SGX523, a small molecule inhibitor of MET. *Invest New Drugs.* 2013; 31:363–9. [PubMed: 22547164]

12. Diamond S, Boer J, Maduskuie TP Jr, Falahatpisheh N, Li Y, Yeleswaram S. Species-specific metabolism of SGX523 by aldehyde oxidase and the toxicological implications. *Drug Metab Dispos.* 2010; 38:1277–85. [PubMed: 20421447]
13. Moriwaki Y, Yamamoto T, Takahashi S, Tsutsumi Z, Hada T. Widespread cellular distribution of aldehyde oxidase in human tissues found by immunohistochemistry staining. *Histol Histopathol.* 2001; 16:745–53. [PubMed: 11510964]
14. Smith DA, Obach RS. Metabolites in safety testing (MIST): considerations of mechanisms of toxicity with dose, abundance, and duration of treatment. *Chem Res Toxicol.* 2009; 22:267–79. [PubMed: 19166333]
15. Pirouzpanah S, Rashidi MR, Delazar A, Razavieh SV, Hamidi A. Inhibitory effects of *Ruta graveolens* L. extract on guinea pig liver aldehyde oxidase. *Chem Pharm Bull (Tokyo).* 2006; 54:9–13. [PubMed: 16394541]
16. Shapiro GI, McCallum S, Adams LM, Sherman L, Weller S, Swann S, et al. A Phase 1 dose-escalation study of the safety and pharmacokinetics of once-daily oral foretinib, a multi-kinase inhibitor, in patients with solid tumors. *Invest New Drugs.* 2013; 31:742–50. [PubMed: 23054208]
17. Gordon MS, Sweeney CS, Mendelson DS, Eckhardt SG, Anderson A, Beaupre DM, et al. Safety, pharmacokinetics, and pharmacodynamics of AMG 102, a fully human hepatocyte growth factor-neutralizing monoclonal antibody, in a first-in-human study of patients with advanced solid tumors. *Clin Cancer Res.* 2010; 16:699–710. [PubMed: 20068101]
18. Spigel DR, Ervin TJ, Ramlau RA, Daniel DB, Goldschmidt JH Jr, Blumenschein GR Jr, et al. Randomized phase II trial of Onartuzumab in combination with erlotinib in patients with advanced non-small-cell lung cancer. *J Clin Oncol.* 2013; 31:4105–14. [PubMed: 24101053]
19. Obach RS, Huynh P, Allen MC, Beedham C. Human liver aldehyde oxidase: inhibition by 239 drugs. *J Clin Pharmacol.* 2004; 44:7–19. [PubMed: 14681337]

Statement of translational relevance

The early clinical testing of novel target specific agents is an important part of improving anti-cancer treatment. Preclinical animal data guide initial clinical safety assumptions, and dogs, mice and rats are the most frequently used species. This first-in-human study with JNJ-38877605 revealed renal toxicity, even at sub-therapeutic doses, that was not predicted by the aforementioned animal models. Subsequently performed rabbit studies showed that species specific metabolism of quinoline ring structures of JNJ-38877605 through aldehyde oxidase resulted in the formation of insoluble metabolites that form crystal structures in the kidney leading to renal toxicity. Our findings suggest that in case of involvement of aldehyde oxidase, rabbit models should be used as alternative toxicology species.

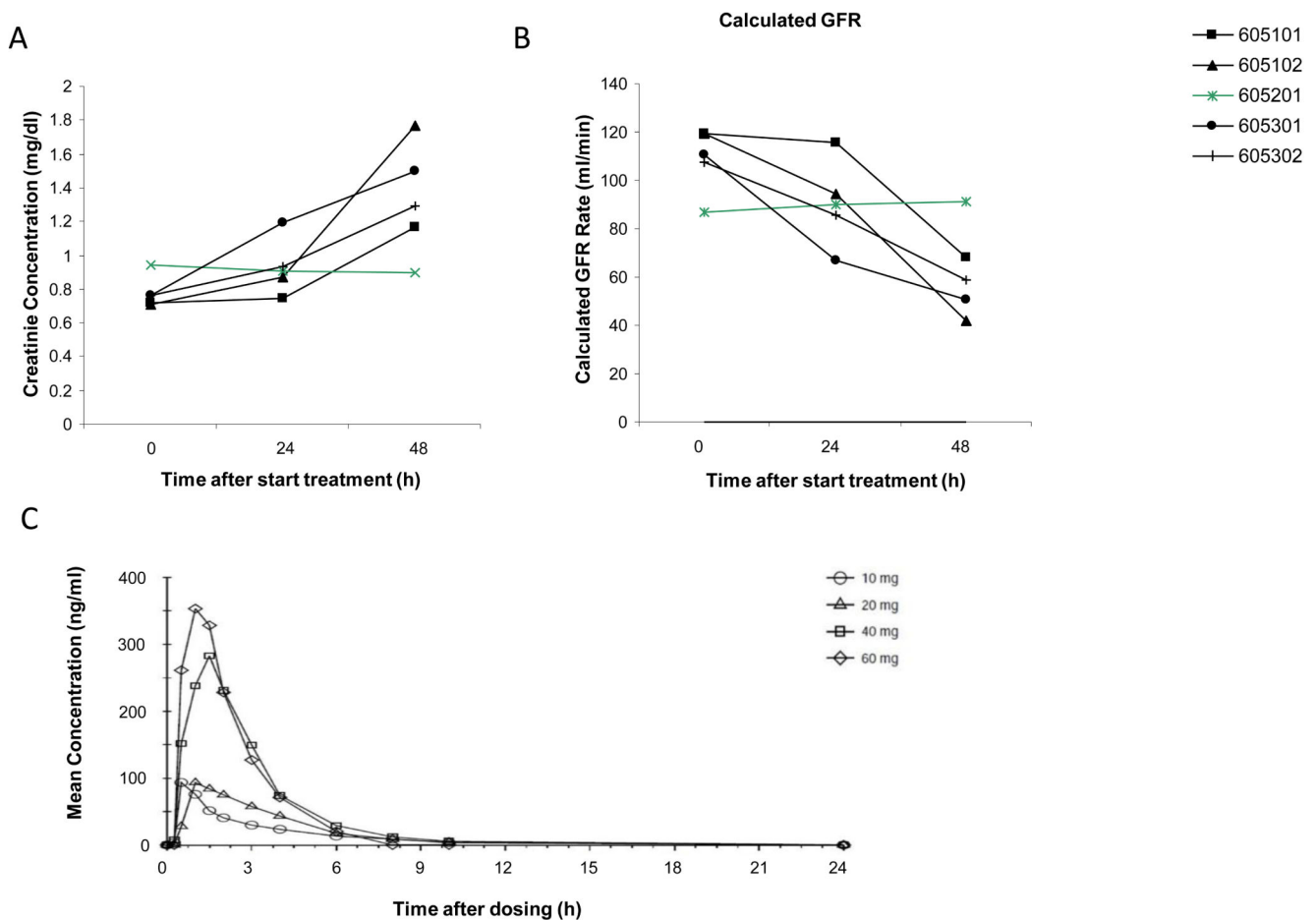


Figure 1.

Renal toxicity in a first-in-human phase I study using JNJ-38877605. A) Serum creatinine levels as collected from each individual in the 60mg JNJ-38877605 over time were plotted. Each line represents an individual patient. B) Calculated creatinine clearance as determined by the Cockcroft-Gould formula at each time-point is plotted. Each line represents an individual patient. C) Human pharmacokinetics of JNJ-38877605 after oral administration on cycle 1 day 1 of the different patient cohorts. Each line represents the mean concentration over time for a dosing cohort.

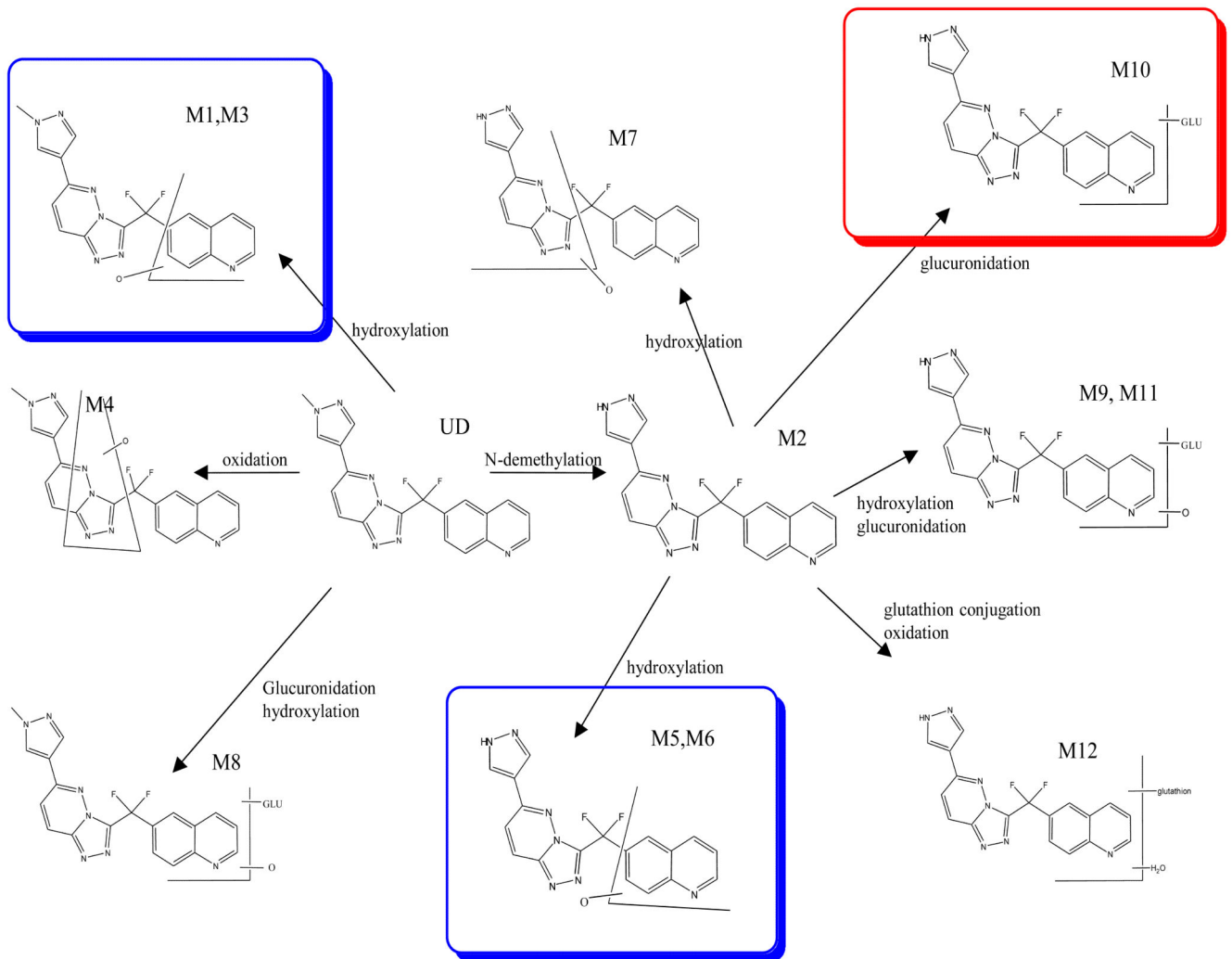


Figure 2. Proposed Metabolic Pathways for JNJ-38877605 Based on In Vitro Incubates of Liver Subcellular Fractions and Hepatocytes rat, rabbit, dog, monkey and man with JNJ 38877605.

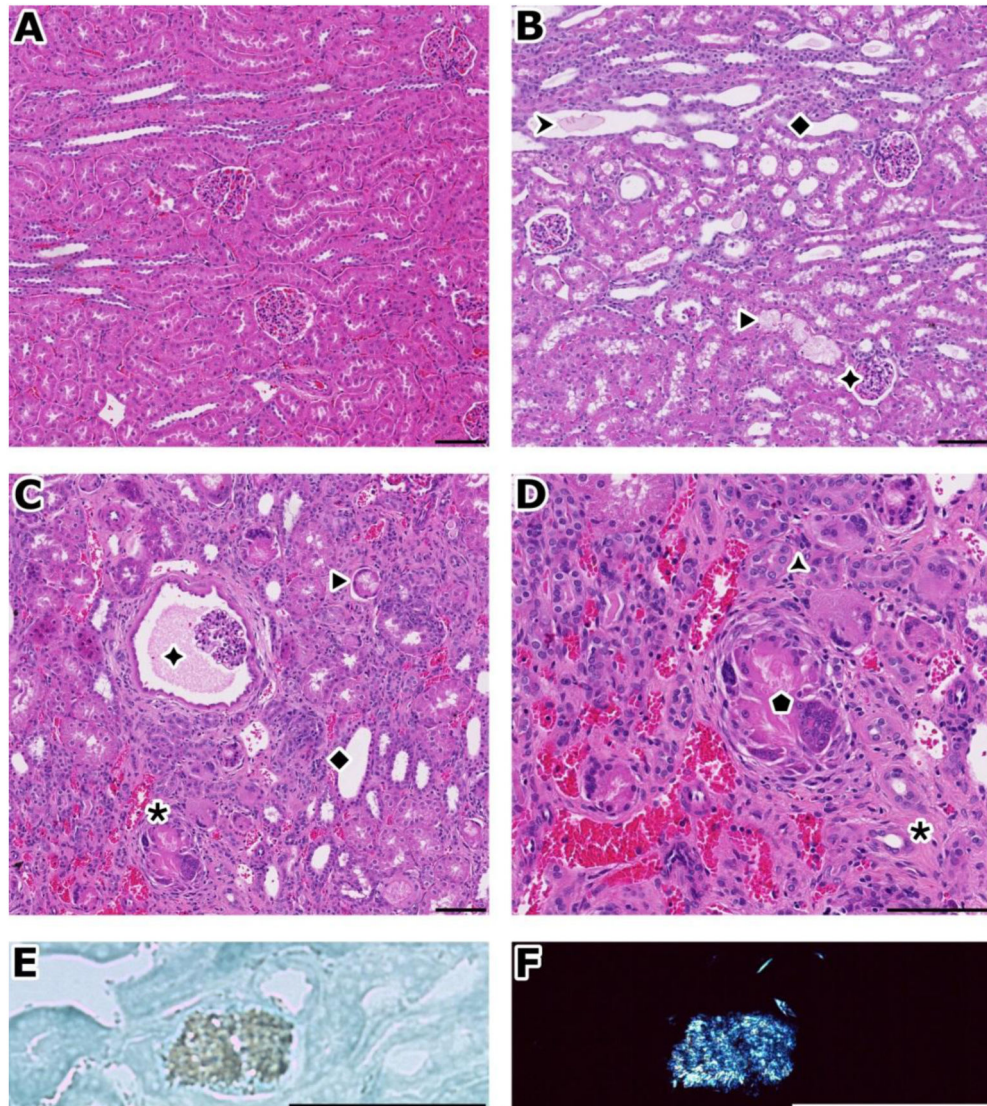


Figure 3.

Pathologic findings of toxicity study in rabbits

A) normal kidney. B) after 7 days, accumulation of granular material (▶) or spicules (◀) in dilated and basophilic corticotubules and collecting ducts (◆). Glomerules are normal (◆). C) after 1 month, there is extensive cortical damage with chronic tubulo-interstitial inflammation (*), see prominent Bowman's space dilation (◆). D) Close up of inflammation from figure C); regenerating tubules (basophilic) with thick basement membrane (▲), diffuse infiltrate (mainly mononuclear), congestion, interstitial fibrosis (*), giant cells around acicular clefts (●). E) Appearance of an acicular crystal under bright field illumination. F) same birefringent crystal than in E), under polarization. This foreign material deposited in tubules forms spicules as in this example or can also be granular. A-C: H&E, original magnification: 10×. D: H&E, original magnification: 20×. E, F: frozen section, methylene blue, original magnification: 40×. Bar: 100 μm

Table 1
noteworthy post-mortem changes – 1-month dosing phase

| Group | | 1 (control) | 2 | 3 | 4 | 5 | 6 |
|---|------------------------|----------------|-------------|----------------|--------------|--------------|--------------------|
| Dosing regimen in mg/kg | | 0 | 50 – 3/week | 100 – 1/week | 200 – 1/week | 100 – 3/week | 50 – 1/day |
| Dose in mg/kg/week | | 0 | 150 | 100 | 200 | 300 | 350 |
| N | | 4 ^a | 4 | 4 ^a | 4 | 4 | 4 |
| Organ weights | | | | | | | |
| Kidney weights | Fold change vs control | 17.23 g | ×0.93 | ×1.31 | ×1.20 | ×1.13 | ×1.16 ^b |
| Microscopy | | | | | | | |
| Dilatation, collecting ducts with amorphous material | Incidence | 0 | 3 | 4 | 4 | 4 | 4 |
| | minimal | | 3 | 1 | 0 | 1 | 0 |
| | slight | | 0 | 3 | 3 | 2 | 2 |
| | moderate | | 0 | 0 | 1 | 1 | 2 |
| Basophilia, corticotubular with basement membrane thickening | Incidence | 0 | 2 | 2 | 4 | 3 | 4 |
| | minimal | | 2 | 0 | 2 | 0 | 2 |
| | slight | | 0 | 2 | 1 | 2 | 0 |
| | moderate | | 0 | 0 | 1 | 1 | 2 |
| Hypertrophy, corticotubular; with spicules and multinucleated cells | Incidence | 0 | 1 | 3 | 4 | 4 | 4 |
| | minimal | | 1 | 1 | 1 | 1 | 2 |
| | slight | | 0 | 2 | 2 | 3 | 2 |
| | moderate | | 0 | 0 | 1 | 0 | 0 |
| Dilation, corticotubular, extending towards cortex | Incidence | 0 | 0 | 0 | 3 | 3 | 3 |
| | minimal | | | | 2 | 2 | 2 |
| | slight | | | | 1 | 1 | 1 |
| Fibrosis, cortical | Incidence | 0 | 0 | 0 | 1 | 2 | 2 |
| | minimal | | | | 0 | 2 | 1 |
| | slight | | | | 1 | 0 | 1 |

^a 1 dead animal (mean kidney weights calculated on 3 values)

^b the right kidney from male 13 was aplastic and the kidney weight change is underestimated in this group

Table 2
Metabolites of JNJ-38877605 in Plasma

| Species | Metabolites | | | | | | | | UD |
|---------|-------------|------|-----|-----|------|------|-----|-----|-------|
| | M1 | M2 | M3 | M4 | M5 | M6 | M7 | M10 | |
| Rat | 136 | | 64 | 57 | 15 | 6 | | | 1466 |
| Dog | 31 | | 55 | 40 | | | | | 575 |
| Rabbit | | 6388 | 778 | 603 | 2259 | 1780 | 395 | 822 | 22836 |
| Man | | 3 | 387 | | 208 | | | 2 | 111 |

The metabolites of JNJ-38877605 were determined in urine/faeces of rat, dog and rabbit and in urine of man. Animals were dosed with 3H-JNJ-38877605 at 2.5 mg/kg in rat, 2.5 mg/kg in dog and 100 mg/kg in rabbit. Humans were dosed at 60 mg. JNJ-38877605 and its metabolites in plasma were expressed as ngeq/ml. Metabolites were measured at about Cmax ranging between 1 and 4h depending on the species. UD=unchanged drug or JNJ-38877605

Table 3
Identification of the enzymes causing generation of the insoluble metabolite M3

| 3a. Formation of metabolites after incubation of JNJ-38877605 with microsomes or 12000 ×g supernatant | | | | | |
|---|-------------------------|--------------------------------------|------|------|--------------------------------------|
| Matrix | metabolites | | | | |
| | M1/M2 | M3 | M4 | UD | |
| Microsomes 12000 ×g | 4.46 | 1.21 | 4.07 | 12.8 | |
| | 2.82 | 24.53 | 1.92 | 26.0 | |
| 5 μM ³ H-JNJ-38877605 was incubated with human liver microsomes or 12000 ×g during 120 min. | | | | | |
| 3b. Inhibition of the metabolism of JNJ-38877605 and the formation of the major metabolites in human liver supernatant by an inhibitor of aldehyde oxidase and cytochrome P-450. | | | | | |
| Inhibitor | Enzyme | M1/M2 | M3 | M4 | UD (sum of all metabolite formation) |
| | | % inhibition of metabolite formation | | | |
| Quercetin | Aldehyde oxidase CYP2C8 | 75 | 94 | 73 | 112 |
| 1-aminobenzotriazole | CYP-450 | 58 | 1 | 70 | 19 |
| 5 μM ³ H-JNJ-38877605 was incubated with human 12000×g liver supernatant. | | | | | |